Altruism, Social Interactions, and the Course of a Pandemic*

Laura Alfaro†
Harvard Business School and NBER

Ester Faia‡
Goethe University Frankfurt and CEPR

Nora Lamersdorf§
Frankfurt School of Finance & Management

Farzad Saidi¶
University of Bonn and CEPR

August 16, 2023

Abstract

Externalities and social preferences, such as altruism, play a key role in the choice of social interactions, which in turn affect the diffusion of a pandemic. We build a dynamic epidemiological model with endogenous social interactions in a frictional environment, also in a variant with heterogeneous agents and a network structure. Taking into account agents' endogenous behavior and altruism generates markedly different predictions relative to a naïve epidemiological model with exogenous contact rates. Congestion and commitment inefficiencies arise, even under full altruism, and call for policy intervention. We derive the efficient allocation, and show how the Ramsey planner can mitigate the respective externalities.

JEL codes: D62, D64, D85, D91, E70, I10, I18

Keywords: social interactions, pandemics, SIR models, social preferences, targeted policies

∗ We thank John Cochrane, Pietro Garibaldi, Maximilian Mayer, Krisztina Molnar, Dirk Niepelt, Vincenzo Pezone and Venky Venkateswaran, as well as multifarious seminar participants for their comments and suggestions. We also thank Christina Brinkmann for excellent research assistance. Saidi's research is funded by the Deutsche Forschungsgemeinschaft (DFG, German Research Foundation) under Germany's Excellence Strategy (EXC 2126/1 – 390838866), and Faia gratefully acknowledges funding by the DFG under grant FA-1022-2. A previous version of the model was circulated as NBER Working Paper No. 27134 under the title "Social Interactions in Pandemics: Fear, Altruism, and Reciprocity."
† E-mail: lalfaro@hbs.edu
‡ E-mail: faia@wiwi.uni-frankfurt.de
§ E-mail: n.lamersdorf@fs.de
¶ E-mail: saidi@uni-bonn.de

1. Introduction

Externalities, positive or negative, may arise naturally in networked communities. Furthermore, societies and cultures exhibit deeply rooted differences in traits such as social preferences (see, among others, Hofstede, 2001; Spolaore and Wacziarg, 2013; Falk et al., 2018). Both affect individuals' choice of social interactions, which in turn governs the extent of network externalities, such as the diffusion of information or an infectious disease. The goal of this paper is to provide a framework that incorporates these behavioral adjustments and to design the optimal policy response, taking into account heterogeneous agents and different community and social traits.

We build a dynamic model in which agents choose the intensity of social interactions. In a frictional environment, they maximize their lifetime utility, which increases with social contacts, while internalizing potential externalities stemming from these social contacts. When agents are altruistic, they also take into account the impact of their behavior on others. We apply our model to the COVID-19 pandemic and show that these behavioral responses directly affect the spread of the disease. In particular, susceptible individuals, aware of their infection risk, voluntarily reduce their social contacts. The intensity of social interactions determines the probability of infection and, thus, the evolution of the number of susceptible, infected, and recovered individuals. We show that agents' behavioral adjustment flattens the infection curve compared to a model with exogenous contact rates, even in the absence of any stringency measures imposed by a social planner.

Motivated by the empirically documented importance of altruism in reducing mobility during the pandemic (Alfaro et al., 2022), we follow Becker (1974) and include an altruistic motive in the lifetime utility of infected individuals,[1] such that they care about the infection risk of their susceptible peers and change their own behavior accordingly. Using analytical results and simulations, we show that a higher degree of altruism helps significantly flatten the infection curve. This is the net outcome of two effects: while altruistic infected agents reduce their social contacts by more, this also allows susceptible agents to decrease their

1 This enables a time-consistent solution to our dynamic problem (as in, e.g., Doepke and Tertilt, 2009).

social activity by less due to the lower infection risk stemming from a decrease in infected agents' social contacts.

We present a network variant of our model with different groups among the susceptible, infected, and recovered. These groups represent individuals who are heterogeneously exposed to the infection risk due to different recovery rates. In this model variant, agents from each group choose the level of social interactions towards all groups individually. In simulations, we illustrate that susceptible individuals belonging to a more vulnerable group reduce their overall social activity by more, and especially so towards members from a potentially more infectious group. Altruistic infected individuals, in turn, reduce their social interactions by more towards members from a more vulnerable group. Again, a higher degree of altruism gives susceptible agents—especially the more vulnerable ones—the possibility to reduce their social interactions by less since part of the burden is carried by the infected agents.

By comparing the decentralized and the social planner's solution, we show that congestion and commitment inefficiencies arise in the former. The (static) congestion inefficiency is dictated by the non-linearities of the matching process and the (dynamic) commitment inefficiency by the failure of atomistic agents to foresee the aggregate future evolution of the disease, which the planner is well aware of.[2] Inefficiencies, in turn, call for policy intervention. As inefficiencies are specific to groups in the network variant of our model, addressing them requires group-targeted policies. From the range of potential policy instruments, we focus on lockdowns, a prominent "corner solution" during the earlier waves of the pandemic. We characterize under what conditions such a stringency policy can achieve efficiency by equalizing the ratio of the marginal utility from social activity for an infected agent and the one for a susceptible agent across the decentralized equilibrium and the efficient solution.

Finally, we quantify the optimal lockdown policy through the simulation of the social planner's solution. A distinctive feature of the planner's lockdown policy is its front-loading, as most of the activity is restricted in the first few periods. In the network model with

2 This is similar to Moser and Yared (2022), in that we highlight dynamic inefficiencies compared to the social planner's commitment.

heterogeneous agents, we show that optimal initial restrictions are stricter for agents that spread the disease more, and later restrictions are stricter for the most vulnerable groups.

Relation to the literature. Our paper contributes to the literature on health externalities and their social consequences. We present a model of endogenous behavior in the face of those externalities that combines a dynamic optimization problem of social interactions with altruistic preferences and a network structure. Spurred by the onset of the COVID-19 pandemic, the literature on the economics of pandemics has evolved fast and now comprises a substantial body of work. As any feasible list would be incomplete at this point, we focus on the subset of papers related to the different ingredients of our model.

Motivated by the fact that neglecting behavioral responses may lead to naïve policy prescriptions, the incorporation of individual decision making is now an important pillar for a host of models. Kremer (1996), Fenichel et al. (2011), and Fenichel (2013) are among the first studies to integrate behavior in an epidemiological model with optimizing agents. This tradition is continued also in the context of the more recent pandemic (see, for instance, Brotherhood et al., 2020; Toxvaerd, 2021; Chakrabarti et al., 2022; Dasaratha, 2022; Rachel, 2022). These papers generally highlight the role of infection externalities associated with contact exposure to infected individuals. Toxvaerd (2019) does so using an SIS model, while Makris (2021) studies private social distancing and—similarly to our model—accounts for heterogeneous infection-induced fatality rates.

Greenwood et al. (2019), Garibaldi et al. (2020a,b), and Farboodi et al. (2021) all study the spread of diseases in a search model. In contrast to Garibaldi et al. (2020a,b) and Farboodi et al. (2021), we differentiate between the behavior of susceptible and infected individuals, and formalize the endogenous social network, as well as its social planner solution, with heterogeneous groups. In the context of HIV, Greenwood et al. (2019) calibrate their model to quantify whether behavioral adjustments affect the effectiveness of policy interventions.[3] In their model, agents can exhibit different degrees of patience.

A key difference of our model is that we consider the role of altruism—i.e., social as opposed to time preferences—which influences interactions in the presence of negative externalities,

3 Chakrabarti et al. (2022), Dasaratha (2022), and Rachel (2022) focus on this issue for the pandemic.

and differentially so when we allow for groups that are heterogeneous in their vulnerability to the externalities. This allows us to examine how altruism shapes social interactions in an endogenous network, including its comparison with a social planner internalizing externalities.

Prosocial preferences[4] have important implications for our setting: the fact that infected individuals internalize the cost of infection for susceptible individuals, and reduce their contacts accordingly, allows the latter to reduce their social interactions by less. We show that even when all agents exhibit the maximum degree of altruism, they fail to fully internalize the externalities, and the level of social interactions of infected individuals remains higher in the decentralized equilibrium than in the social planner's solution. This constitutes, to the best of our knowledge, a novel result in the literature.

Among the few papers that incorporate a role for altruism is Farboodi et al. (2021). However, their solution under full altruism is equivalent to the social planner's solution, which does not hold in our discrete-time version of a search-theoretical framework that allows us to carve out the role of dynamic inefficiencies.

Furthermore, Toxvaerd (2021) considers the role of altruism in a game-theoretic epidemiological model. While he studies different types of contacts, we consider groups of agents that differ in their recovery rates, and furthermore add dynamic considerations. Brotherhood et al. (2020) model altruism in an epidemiological model as a preference for staying at home. In our model, the utility of altruistic infected individuals depends directly on that of susceptible individuals, leading the former to internalize the externalities of their behavior.

Our result that the decentralized equilibrium is inefficient even when agents are fully altruistic motivates the incorporation of heterogeneous agents that are differentially affected by the remaining externalities. In contrast to the above-mentioned models with optimizing heterogeneous agents (e.g., Makris, 2021), we introduce an endogenous network allowing for meaningful interactions among such heterogeneous groups. Our model variant with heterogeneous agents is related to recent work on models of transmission through networks, showing how the structure of networks may affect the dynamics of the epidemic diffusion

4 Prosocial behavior and, specifically, altruism have been studied in several forms, ranging from warm-glow preferences to unconditional altruism (see Becker, 1974; Andreoni, 1989, 1993; Bolton and Ockenfels, 2000; Andreoni and Miller, 2002; Frey and Meier, 2004).

(Keeling and Eames, 2005). These epidemiological networks tend to be static, not allowing for changes in the network structure. Models with such exogenous networks are reviewed in, for instance, Kiss et al. (2017) and Newman (2018).

A notable exception featuring endogenous networks is Talamàs and Vohra (2020), who study an epidemiological model in which agents strategically choose their partners, but with limited heterogeneity of agents and their interactions. In contrast, we propose an endogenous network model in which agents solve dynamic optimization problems and choose their social interactions vis-à-vis their own and each other group.[5] In the context of a pandemic that affects agents differentially, the incorporation of heterogeneous groups and allowing them to interact with one another are crucial for the optimal policy response.

Acemoglu et al. (2021) study the spread of the pandemic in a network with heterogeneous groups, but links are exogenous and social preferences are absent. In our model, altruistic infected individuals reduce their contacts by more towards members of a more vulnerable segment of the population. This leads to an even greater flattening of the infection curve.

More generally, while we devise an application to the pandemic, our theory builds on a class of models in which agents make a costly contact-intensity choice in a frictional market. There are prominent applications of these models to goods markets (see Rubinstein and Wolinsky, 1987) or financial markets (see Duffie et al., 2005; or, more recently, Farboodi et al., 2023). Closer to ours are models that study endogenous social-network formation within a search-theoretical framework. Endogenous social interactions were first formalized in an equilibrium model by Brock and Durlauf (2001). The impact of social interactions on social structures is covered by Case and Katz (1991) and Glaeser et al. (1996). Currarini et al. (2009) study the formation of social ties through utility maximization, and show the emergence of homophily through a biased search and matching process. Cabrales et al. (2011) provide a tractable model where both socialization (or network formation) and productive efforts can be analyzed simultaneously.

Overall, and relative to the state of the literature, the key innovation of our paper consists

5 In this regard, our model is related to Wu and Shimer (2021), who apply an endogenous network model to the pandemic without an altruistic motive but analyzing strategic complementarities in matching.

of combining a dynamic optimization problem of social interactions within a search-theoretical model with altruistic preferences and a variant featuring a network structure. The dynamic optimization problem is crucial to assess the role of dynamic externalities, altruistic preferences allow, among others, for a comparison with the social planner's solution, and the network structure accounts for realistic and meaningful heterogeneity in interactions.

2. A Model of Endogenous Social Interactions and Altruism

2.1. Baseline Model

Model setup. In our model, time is discrete and there is an infinite horizon. In the baseline model, all agents are of the same types, but can be in three different states: susceptible (S), infected (I), or recovered (R). Later, we extend the model to three age groups, featuring different recovery rates. Transitions of susceptible individuals from state S to I depend on contacts with other people.[6]

Each representative agent has an additively separable per-period utility function $U(x^i_{s,t}) = u(x^i_{s,t}) - c(x^i_{s,t})$, where $x^i_{s,t}$ denotes social activities at time t and $i \in \{S, I, R\}$. $u(x^i_{s,t})$ is increasing in its argument and the cost function, $c(x^i_{s,t})$, puts a constraint on the choice of social activities. We assume that the per-period utility function is concave with $\frac{\partial^2 U(x^i_{s,t})}{\partial^2 x^i_{s,t}} < 0$. Note that the instantaneous utility function may also include other arguments, which we neglect for the sake of exposition.

At time t, a susceptible agent enjoys the per-period utility, expects to enter the infected state in the next period with probability p_t or to remain susceptible with probability $(1 - p_t)$, and chooses the amount of social activities. In doing so, she recognizes that her own social activity increases the risk of infection, taking as given the social activity of others and the

6 Transitions of individuals in the infected group, I, to recovery, R, depend only on medical conditions related to the disease (mostly the healthcare system) that are outside of an individual's control.

aggregate states of the disease. The value function of a susceptible individual reads as follows:

$$V_t^S = U(x_{s,t}^S) + \beta[p_t V_{t+1}^I + (1 - p_t)V_{t+1}^S], \tag{1}$$

where β is the time discount factor and captures the agent's degree of patience, and V_t^I is the value function of an infected individual. The latter is given by:

$$V_t^I = U(x_{s,t}^I) - C^I + \beta[(1 - \gamma)V_{t+1}^I + \gamma V_{t+1}^R] + \delta S_t V_t^S, \tag{2}$$

where C^I is a cost that individuals incur while being infected. Infected individuals remain so for an additional period with probability $(1 - \gamma)$ or recover with probability γ. They might care about their susceptible peers, of which there are S_t. Therefore, the parameter δ captures the degree of altruism and puts a weight on the lifetime utility of susceptible individuals, multiplied by their population share.[7]

Assumption 1. *There exists a combination of parameter values for the cost C^i, the recovery rate γ, the degree of altruism δ, and the disease transmission rate η (specified below) such that $V_t^I - V_t^S < 0 \ \forall t$ for any admissible value of $x_{s,t}^S$.*

The value function of recovered individuals reads as follows: $V_t^R = U(x_{h,t}^R, x_{s,t}^R) + \beta V_{t+1}^R$, as once they have recovered, they are immune to a new infection. Finally, the contact probability p_t determines the infection rate in the classical SIR system:

$$S_{t+1} = S_t - p_t S_t; \qquad I_{t+1} = I_t + p_t S_t - \gamma I_t; \qquad R_{t+1} = R_t + \gamma I_t, \tag{3}$$

where S_t, I_t, and R_t denote the total share/number of susceptible, infected, and recovered individuals, respectively, at time t and $S_t + I_t + R_t = N_t \equiv 1 \ \forall t$.[8]

Matching function, geography, and infection probability. The number of contacts

7 Such a setup implicitly assumes that agents recognize their symptoms. However, extending our model to incorporate asymptomatic cases would not affect the main channels that we discuss.

8 Note that the exogenous contact rate in the classical SIR model, which is presented in Appendix E where we also briefly describe its limitations, relates to our infection probability as follows: $p_t = \lambda I_t$, where λ is assumed to be constant and exogenously given.

per individual depends on a matching process along the lines of Diamond (1982) or Pissarides (2000). The intensity of social interactions, $x^i_{s,t}$ for $i \in \{S, I, R\}$, can be defined as the number of times an individual leaves her home or the probability of doing so per unit of time. In the course of these social activities, agents come in contact with other individuals. The number of contacts depends on the average level of social activity in the population, $\bar{x}_{s,t}$. Normalizing the population size to 1, the latter is given by $\bar{x}_{s,t} = S_t \bar{x}^S_{s,t} + I_t \bar{x}^I_{s,t} + R_t \bar{x}^R_{s,t}$, where $\bar{x}^S_{s,t}$, $\bar{x}^I_{s,t}$, and $\bar{x}^R_{s,t}$ are the average levels of social activity of susceptible, infected, and recovered individuals, respectively.

The total number of contacts for the average level of social activity depends on the matching function $m(\bar{x}_{s,t}) = (\bar{x}_{s,t})^\alpha$. The parameter α captures the returns to scale, which serves as a proxy for geographical properties. Cities with denser logistical structures induce more overall contacts per social activity.[9] The average number of contacts per social activity is then given by $\frac{m(\bar{x}_{s,t})}{\bar{x}_{s,t}} = (\bar{x}_{s,t})^{\alpha-1}$. By multiplying the latter with the susceptible individual's chosen level of social activity, we obtain the overall number of contacts of a susceptible agent $x^S_{s,t}(\bar{x}_{s,t})^{\alpha-1}$. Furthermore, the infection probability depends on the chosen level of social activity by infected individuals, $x^I_{s,t}$, and the overall number of infected individuals, I_t. Hence, the infection probability in the decentralized equilibrium is given by

$$p_t(\cdot) = \eta x^S_{s,t} x^I_{s,t} \frac{m(\bar{x}_{s,t})}{\bar{x}_{s,t}} I_t = \eta x^S_{s,t} x^I_{s,t} (\bar{x}_{s,t})^{\alpha-1} I_t, \tag{4}$$

where $\eta > 0$ is an exogenous transmission rate. If $\alpha = 0$, the probability $p_t = \eta x^S_{s,t} x^I_{s,t} \bar{x}^{-1}_{s,t} I_t$ is homogeneous of degree one, implying constant returns to scale, while if $\alpha = 1$, the probability becomes a quadratic function (see Diamond, 1982), exhibiting increasing returns to scale. Note that atomistic agents take the level of social interactions of other agents as given.

Optimality conditions. Susceptible agents' first-order condition with respect to $x_{s,t}$ is:

$$\frac{\partial U(x^S_{h,t}, x^S_{s,t})}{\partial x^S_{s,t}} + \beta \frac{\partial p_t(\cdot)}{\partial x^S_{s,t}} (V^I_{t+1} - V^S_{t+1}) = 0. \tag{5}$$

9 For instance, Brotherhood et al. (2022) show how urban density can shape the dynamics of a pandemic.

Susceptible individuals internalize the drop in utility associated with the risk of infection and—given Assumption 1 and the shape of the utility function—choose a lower level of social activity than they would in the absence of a pandemic. In line with empirical evidence in Alfaro et al. (2022), a higher discount factor β, capturing a higher level of patience, curbs social activity by more. The first-order condition of infected agents with respect to $x_{s,t}$ is:

$$\frac{\partial U(x^I_{h,t}, x^I_{s,t})}{\partial x^I_{s,t}} + \delta S_t \beta \frac{\partial p_t(\cdot)}{\partial x^I_{s,t}} (V^I_{t+1} - V^S_{t+1}) = 0. \tag{6}$$

Finally, the first-order condition of the recovered individuals is: $\frac{\partial U(x^R_{h,t}, x^R_{s,t})}{\partial x^R_{s,t}} = 0$. Recovered individuals, assuming that they are immune to another infection, choose the same level of social activity as they would in the absence of a pandemic. In contrast to recovered individuals, susceptible and altruistic infected ones have incentives that involve a dynamic component, which depends on the infection risk.

Definition 1. *A decentralized equilibrium is a sequence of state variables S_t, I_t, R_t, a set of differentiable and bounded value functions V^S_t, V^I_t, V^R_t, an infection probability p_t, and a sequence of social activities $x^S_{s,t}, x^I_{s,t}, x^R_{s,t}$ such that:*

1. *S_t, I_t, R_t solve* (3)*, with the probability of infection, p_t, given by* (4)*.*
2. *The sequence $x^S_{s,t}, x^I_{s,t}, x^R_{s,t}$ solves* (5)*,* (6)*, as well as $\frac{\partial U(x^R_{s,t})}{\partial x^R_{s,t}} = 0$.*

Note that underlying the decentralized economy is a symmetric Nash equilibrium in the choice of social activity.

The role of altruism. Infected individuals internalize the impact of their decisions on the infection risk for others based on their degree of altruism, which is given by $\delta \in [0, 1]$. If the latter is 0, infected individuals do not internalize the effects of their activity on others, and their first-order condition becomes $\frac{\partial U(x^I_{h,t}, x^I_{s,t})}{\partial x^I_{s,t}} = 0$. In this case, given the concavity of the utility function and Assumption 1, their level of social activity is higher than the one solving (6) with $\delta > 0$. Since the level of social activity of the infected individuals affects the overall infection rate, their degree of altruism is crucial in determining the overall disease

transmission and affects the behavior of susceptible individuals. The following proposition formalizes this finding.

Proposition 1. *Social activity of infected individuals, $x^I_{s,t}$, declines with the degree of altruism, and social activity of susceptible individuals, $x^S_{s,t}$, increases with it.*

Proof. See Appendix A.1.

If infected individuals behave more cautiously due to altruism, the infection probability falls, allowing susceptible individuals to have more social interactions. In addition, in Section 3, we show that the presence of altruism leads to a lower number of infected individuals overall, thereby flattening the infection curve.

2.2. Endogenous Network Model

Within communities, there are heterogeneous groups that differ along several dimensions and interact with one another. Individuals of each one of these groups optimally choose their level of social interactions vis-à-vis their own and each other group, taking as given the actions of others. This extends the notion of a Nash equilibrium to the entire network. In this framework, interactions are again fully endogenous and depend on the states (S, I, R) within each group and the actions of others.[10]

Applying our analysis to the pandemic, we assume that groups differ in terms of their recovery rates, γ^j, which can vary, for instance, across age groups. Each susceptible individual of group j experiences a certain number of contacts per social activity with infected individuals of her own group but also of the other groups. We denote by $\hat{x}^j_{s,t}$ group j's social interactions at time t. The matching function for each group j reads as follows: $m^j(\hat{x}^j_{s,t}) = \left(\sum_k (\bar{x}^{S,jk}_{s,t} + \bar{x}^{I,jk}_{s,t} + \bar{x}^{R,jk}_{s,t})(\bar{x}^{S,k}_{s,t} S^k_t + \bar{x}^{I,k}_{s,t} I^k_t + \bar{x}^{R,k}_{s,t} R^k_t)\right)^{\alpha}$, where $\bar{x}^{S,jk}_{s,t}$, $\bar{x}^{I,jk}_{s,t}$, and $\bar{x}^{R,jk}_{s,t}$ are the respective average intensities of social activity between (each) group j and group k with $k = 1, ..., J$ and $\bar{x}^{i,k}_{s,t} = \sum_j \bar{x}^{i,kj}_{s,t}$ for $i \in \{S, I, R\}$.

The probability of infection for a susceptible person in group j who comes in contact with

10 Appendix F presents an intermediate version of the model in which optimizing agents choose the general level of social activity, while the cross-group links are exogenous.

infected individuals in all groups k is $p_t^j(\cdot) = \sum_k \eta x_{s,t}^{S,jk} x_{s,t}^{I,kj} \frac{m^j(\hat{x}_{s,t}^j)}{\hat{x}_{s,t}^j} I_t^k$. The dynamics of the different states S, I, and R are as described above, but now separately for each group, where now $S_t^j + I_t^j + R_t^j = N_t^j$ and $\sum_j N_t^j \equiv 1 \; \forall t$. The first-order condition for the social activity of susceptible individuals belonging to group j vis-à-vis group k is:

$$\frac{\partial U(x_{s,t}^{S,jk})}{\partial x_{s,t}^{S,jk}} + \beta\eta x_{s,t}^{I,kj} \frac{m^j(\hat{x}_{s,t}^j)}{\hat{x}_{s,t}^j} I_t^k (V_{t+1}^{I,j} - V_{t+1}^{S,j}) = 0. \tag{7}$$

Note that now we have J^2 such first-order conditions. Similarly, for infected individuals with altruistic preferences, the first-order condition with respect to social interactions of each such individual j with agents in any other group k is:

$$\frac{\partial U(x_{s,t}^{I,jk})}{\partial x_{s,t}^{I,jk}} + \delta \frac{S_t^k}{N_t^k} \beta\eta x_{s,t}^{S,kj} \frac{m^k(\hat{x}_{s,t}^k)}{\hat{x}_{s,t}^k} I_t^j (V_{t+1}^{I,k} - V_{t+1}^{S,k}) = 0. \tag{8}$$

The first-order conditions for social interactions of the recovered individuals are the same as in the baseline model, but separately for each group j vis-à-vis each group k.

Definition 2. *A decentralized equilibrium for the endogenous network model with a differential choice of group interactions is equivalent to Definition 1, but for each group j of the population. The J^2 equations* (7) *and* (8) *replace the previous first-order conditions* (5) *and* (6) *and the J^2 equations $\frac{\partial U(x_{s,t}^{R,jk})}{\partial x_{s,t}^{R,jk}} = 0$ replace $\frac{\partial U(x_{s,t}^{R})}{\partial x_{s,t}^{R}} = 0$.*

Corollary 1. *Social activity of susceptible agents of group j vis-à-vis any group k is smaller if there are many infected agents in group k.*

Proof. From the first-order condition (7) it becomes clear that with $V_{t+1}^{I,j} - V_{t+1}^{S,j} < 0$, a larger I_t^k—given the social activity of infected agents $x_{s,t}^{I,kj}$ and the average social activities—leads to a larger marginal utility $\frac{\partial U(x_{h,t}^{S,j}, x_{s,t}^{S,jk})}{\partial x_{s,t}^{S,jk}}$. Due to the concavity of the utility function, this leads to a decrease in $x_{s,t}^{S,jk}$.

Intuitively, if an individual of group j is aware that in group k the share of infected individuals is high, it will reduce the contact with members of that group in order to avoid infection.

Corollary 2. *Social activity of altruistic infected agents of group j vis-à-vis any group k is smaller if the recovery rate of agents in group k is smaller.*

Proof. Suppose there are two agents, k and k', with different recovery rates, $\gamma^k < \gamma^{k'}$. Agent k, hence, remains longer in the infected state, paying the infection cost, so that $V_t^{I,k} - V_t^{S,k} < V_t^{I,k'} - V_t^{S,k'}$. Therefore, the second term in equation (8) is smaller for social interactions with agents of group k, implying a higher marginal utility, $\frac{\partial U(x_{s,t}^{I,jk})}{\partial x_{s,t}^{I,jk}} > \frac{\partial U(x_{s,t}^{I,jk'})}{\partial x_{s,t}^{I,jk'}}$, and a lower level of social activity vis-à-vis agents of group k, $x_{s,t}^{I,jk} < x_{s,t}^{I,jk'}$.

Corollary 2 states that altruistic infected agents behave more cautiously towards susceptible agents of a more vulnerable group. We further validate our findings using simulations in Section 3.

2.3. Social Planner

In the decentralized equilibrium, each individual takes as given the average level of social activity and the future course of the number of susceptible and infected individuals. In contrast, a social planner takes both into account when deciding on her policies. We now draw the comparison between the decentralized equilibrium and the solution to the planner's problem for both models described above.

Baseline model. There is complete information, and the planner knows that in a Nash equilibrium each agent in state i chooses the same amount of social activities, so that $x_{s,t}^i = \bar{x}_{s,t}^i$ for $i \in \{S, I, R\}$. The equilibrium infection rate is then given by: $p_t^P(\cdot) = \eta x_{s,t}^S x_{s,t}^I (S_t x_{s,t}^S + I_t x_{s,t}^I + R_t x_{s,t}^R)^{\alpha-1} I_t$. The social planner chooses the paths of social activities for each agent by maximizing the weighted sum of the lifetime utilities of all agents. The planner is aware of the dependence of the value function of susceptible individuals on the total share of infected and susceptible individuals. We define the value functions in the planner economy as $\hat{V}_t^i$ for $i \in \{S, I, R\}$. The planner chooses the sequence: $[S_{t+1}, I_{t+1}, R_{t+1}, x_{s,t}^S, x_{s,t}^I, x_{s,t}^R]_{t=0}^{\infty}$ at any initial period t to maximize

$$\hat{V}_t^N = S_t \hat{V}_t^S(S_t, I_t) + I_t \hat{V}_t^I + R_t \hat{V}_t^R \tag{9}$$

with $\hat{V}_t^S(S_t, I_t) = U(x_{s,t}^S) + \beta[p_t^P(\cdot)\hat{V}_{t+1}^I + (1-p_t^P(\cdot))\hat{V}_{t+1}^S]$, $\hat{V}_t^I = U(x_{s,t}^I) - C^I + \beta[(1-\gamma)\hat{V}_{t+1}^I + \gamma\hat{V}_{t+1}^R]$, $\hat{V}_t^R = U(x_{s,t}^R) + \beta\hat{V}_{t+1}^R$, and subject to

$$S_{t+1} = S_t - p_t^P(\cdot)S_t, \qquad I_{t+1} = I_t + p_t^P(\cdot)S_t - \gamma I_t, \qquad R_{t+1} = R_t + \gamma I_t, \tag{10}$$

where $S_t + I_t + R_t = N_t \equiv 1 \; \forall t$.

In the social planner's problem, we set $\delta = 0$ since infected agents know that the planner takes into account all the externalities.[11] The first-order condition for recovered individuals' social activities is equivalent to the one obtained in the decentralized equilibrium. The social activities of susceptible and infected individuals are instead given by:

$$\frac{\partial U(x_{s,t}^S)}{\partial x_{s,t}^S} + \beta\frac{\partial p_t^P(\cdot)}{\partial x_{s,t}^S}(\hat{V}_{t+1}^I - \hat{V}_{t+1}^S) + \beta(1-p_t^P(\cdot))\left(\frac{\partial \hat{V}_{t+1}^S}{\partial S_{t+1}}\frac{\partial S_{t+1}}{\partial x_{s,t}^S} + \frac{\partial \hat{V}_{t+1}^S}{\partial I_{t+1}}\frac{\partial I_{t+1}}{\partial x_{s,t}^S}\right) = 0 \tag{11}$$

$$I_t\frac{\partial U(x_{s,t}^I)}{\partial x_{s,t}^I} + S_t\left[\beta\frac{\partial p_t^P(\cdot)}{\partial x_{s,t}^I}(\hat{V}_{t+1}^I - \hat{V}_{t+1}^S) + \beta(1-p_t^P(\cdot))\left(\frac{\partial \hat{V}_{t+1}^S}{\partial S_{t+1}}\frac{\partial S_{t+1}}{\partial x_{s,t}^I} + \frac{\partial \hat{V}_{t+1}^S}{\partial I_{t+1}}\frac{\partial I_{t+1}}{\partial x_{s,t}^I}\right)\right] = 0. \tag{12}$$

Proposition 2. *Suppose $\alpha = 1$. Given the states, the social planner chooses a lower level of social interactions of infected individuals than in the decentralized equilibrium only if the total share of susceptible individuals is positive, that is, $S_t > 0$. This holds even for a maximum level of altruism, $\delta = 1$.*

Proof. See Appendix A.2.

In our fully dynamic equilibrium model with an infinite horizon, a closed-form analytical solution is not obtainable as the levels of social activity depend on the future value functions. Therefore, to compare the levels of social activity in the social planner's solution and the decentralized equilibrium, we compare the first-order conditions that these levels of social activity solve, and infer the latter's qualitative differences across the two regimes. We present this comparison in Appendix A.2. The difference between these first-order conditions indicates

11 All of our results continue to hold, and are in fact reinforced, if $\delta > 0$.

the extent of the externalities that atomistic agents do not internalize in the decentralized equilibrium, which we discuss in the following corollary.

Corollary 3. *The inefficiencies in the decentralized equilibrium can be decomposed into a static inefficiency,*

$$\Phi_t^S = \beta \left[\frac{\partial p_t^P(\cdot)}{\partial x_{s,t}^S} - \frac{p_t(\cdot)}{x_{s,t}^S} \right] (\hat{V}_{t+1}^I - \hat{V}_{t+1}^S) \tag{13}$$

$$\Phi_t^I = \beta \left[\frac{S_t}{I_t} \frac{\partial p_t^P(\cdot)}{\partial x_{s,t}^I} - \delta S_t \frac{p_t}{x_{s,t}^I} \right] (\hat{V}_{t+1}^I - \hat{V}_{t+1}^S), \tag{14}$$

where $\frac{p_t(\cdot)}{x_{s,t}^i} = \frac{\partial p_t(\cdot)}{\partial x_{s,t}^i}$ *for* $i \in \{S, I\}$*, and a dynamic inefficiency,*

$$\Psi_t^S = \beta(1 - p_t^P(\cdot)) \left(\frac{\partial \hat{V}_{t+1}^S}{\partial S_{t+1}} \frac{\partial S_{t+1}}{\partial x_{s,t}^S} + \frac{\partial \hat{V}_{t+1}^S}{\partial I_{t+1}} \frac{\partial I_{t+1}}{\partial x_{s,t}^S} \right) \tag{15}$$

$$\Psi_t^I = \beta \frac{S_t}{I_t} (1 - p_t^P(\cdot)) \left(\frac{\partial \hat{V}_{t+1}^S}{\partial S_{t+1}} \frac{\partial S_{t+1}}{\partial x_{s,t}^I} + \frac{\partial \hat{V}_{t+1}^S}{\partial I_{t+1}} \frac{\partial I_{t+1}}{\partial x_{s,t}^I} \right). \tag{16}$$

The static inefficiency is a classical congestion externality due to the fact that atomistic agents do not internalize the impact of their decisions on the average level of social interactions. Its size is affected by the degree of altruism and by the matching function's returns to scale. In societies with non-altruistic agents or in dense cities, the disease spreads faster in the absence of a central planner, and the size of the inefficiency is larger.

The dynamic inefficiency arises since the planner acts under commitment, and takes into account that the next period's number of susceptible and infected individuals will affect the value function of susceptible individuals through future infection rates. The dynamic inefficiency consists of an *immunity* externality (the first term in the large parentheses) and a *contagion* externality (the second term in the large parentheses), similar to those in Garibaldi et al. (2020a). In principle, these externalities push the optimal level of social activity in opposite directions with the first term being positive and the second one negative. In Appendix A.2 (specifically, in equations (21)-(23)), we show that in our case the contagion externality dominates, leading to a lower level of social activity under the central planner.

Regarding the role of altruism, it follows immediately that:

Corollary 4. *The degree of altruism reduces the size of the static inefficiency.*

Equation (14) reveals that a higher degree of altruism, i.e., a larger δ, reduces the size of the static inefficiency, as it induces infected agents to internalize the cost of their actions on others. However, even a maximum degree of altruism ($\delta = 1$) cannot eliminate the static inefficiency. Importantly, the presence of altruism cannot eliminate the dynamic inefficiency either: the latter depends on the ability to internalize the impact of social interactions on the future evolution of the disease, which is only known to the planner.

Endogenous network model. In the endogenous network model, the social planner chooses the sequence $[S_{t+1}^j, I_{t+1}^j, R_{t+1}^j, x_{h,t}^{S,j}, x_{h,t}^{I,j}, x_{h,t}^{R,j}, x_{s,t}^{S,jk}, x_{s,t}^{I,jk}, x_{s,t}^{R,jk}]_{t=0}^{\infty}$ $\forall k$ at any initial period t and for all j to maximize

$$\hat{V}_t^N = \sum_j (S_t^j \hat{V}_t^{S,j} + I_t^j \hat{V}_t^{I,j} + R_t^j \hat{V}_t^{R,j}). \tag{17}$$

The contact probabilities are given by

$$p_t^{Pj}(\cdot) = \sum_k \eta x_{s,t}^{S,jk} x_{s,t}^{I,kj} \frac{m^j \left(\sum_k (x_{s,t}^{S,jk} + x_{s,t}^{I,jk} + x_{s,t}^{R,jk})(\bar{x}_{s,t}^{S,k} S_t^k + \bar{x}_{s,t}^{I,k} I_t^k + \bar{x}_{s,t}^{R,k} R_t^k) \right)}{\sum_k (x_{s,t}^{S,jk} + x_{s,t}^{I,jk} + x_{s,t}^{R,jk})(\bar{x}_{s,t}^{S,k} S_t^k + \bar{x}_{s,t}^{I,k} I_t^k + \bar{x}_{s,t}^{R,k} R_t^k)} I_t^k, \tag{18}$$

with $k = 1, ..., J$ and $\bar{x}_{s,t}^{i,k} = \sum_j x_{s,t}^{i,kj}$ for $i \in \{S, I, R\}$. The first-order conditions for the levels of social activity of susceptible and infected agents in each group j vis-à-vis group k, i.e., $x_{s,t}^{S,jk}$ and $x_{s,t}^{I,jk}$, are reported in Appendix B.

Proposition 3. *Suppose $\alpha = 1$. The social planner chooses a lower level of social interactions of infected individuals of group j vis-à-vis group k than in the decentralized equilibrium only if $\delta I_t^j < N_t^k$, that is, if the number of infected agents in group j multiplied by their level of altruism is smaller than the total population in group k.*

Proof. See Appendix A.3.

Proposition 3 implies that as long as the share of infected agents in group j is smaller than the overall population in group k, the social planner reduces the level of social activity of

infected individuals of group j vis-à-vis group k compared to the decentralized equilibrium even if in the latter agents exhibit the maximum level of altruism. Relative inefficiencies arise also in the network model since the intensity of social activity across groups depends on heterogeneous, group-specific preferences and risk. For example, altruism can now induce a greater (smaller) reduction of contacts towards more (less) vulnerable groups.

Policy implementation. The presence of inefficiencies can be addressed by means of a policy implementation. We focus on the role of general lockdown policies, namely the fraction of mandatory restricted social activity of susceptible, infected, and recovered agents, θ. We refer to the ratio of the marginal utility from social activity for an infected agent and the one for a susceptible agent as the marginal rate of substitution between one infected and one susceptible agent.

Proposition 4. *The marginal rates of substitution between one infected and one susceptible agent in the decentralized and in the social planner's equilibrium become equivalent if the planner sets a stringency measure θ so as to equalize the infection probabilities across the two equilibria, that is:*

$$p_t(\theta, \cdot) = \eta(1-\theta)x^S_{s,t}(1-\theta)x^I_{s,t}\frac{m((1-\theta)\bar{x}_{s,t})}{(1-\theta)\bar{x}_{s,t}}I_t. \tag{19}$$

Proof. See Appendix A.4.

If the infection probabilities are equal in the two equilibria, the static inefficiency is eliminated under full altruism, $\delta = 1$. Beyond that, if the social planner's infection probabilities are enforced under the decentralized equilibrium, the dynamic inefficiency is eliminated as well, as the dynamic of the pandemic follows the one in the social planner's solution.

3. Quantitative Analysis

In this section, we simulate the two variants of our model. After ascertaining the impact of social-activity choices on the infection dynamics, we demonstrate the importance of altruism

in shaping agents' behavior and flattening the infection curve, and confirm our analytical findings for both the baseline and the endogenous network model. Finally, we illustrate the solutions under a central planner and quantify the role of optimal lockdown policies implemented by a Ramsey planner, who takes as given the optimizing conditions of agents.

Calibration. The instantaneous utility of susceptible and infected individuals is a function of their social activities $x^S_{s,t}$ and $x^I_{s,t}$, respectively.[12] The functional forms read as follows: $U(x^S_{s,t}) = c_S \log(x^S_{s,t}) - x^S_{s,t} + 1$ and $U(x^I_{s,t}) = c_I \log(x^I_{s,t}) - x^I_{s,t} + 1$ for susceptible and infected individuals. c_S and c_I denote the respective steady-state levels of social activity, which we set equal to 1. The infection cost C_I is calibrated based on the infection fatality rate and the value of a statistical life (VSL).[13]

We set $\alpha = 1$, implying a quadratic matching function. The recovery rate γ is 1/10. The implied infection duration of 10 days matches different quarantine rules applied in reality and considered in other papers simulating the COVID-19 pandemic.[14] In the endogenous network model, we consider three age groups that differ in their recovery rates (similar to Acemoglu et al., 2021): the young ($20-49$ years), middle-aged ($50-64$ years), and old (65+ years) with respective population shares of $N_y = 53\%$, $N_m = 26\%$, and $N_o = 21\%$. Their recovery rates are such that young agents recover faster: $\gamma_y = 1/7$, $\gamma_m = 1/10$, and $\gamma_o = 1/14$. The disease transmission rate η is chosen so as to match a basic reproduction number $R_0 = \frac{\eta}{\gamma}$ of 2.5.[15] The degree of altruism δ is between 0 and 1, and set to 0.5 in our baseline simulations. The discount factor β is set to 0.99. The economy is initially in a steady state with no infections. An MIT shock increases the total share of infected agents from 0 to $\epsilon = 0.0001 = 0.01\%$ (see Brotherhood et al., 2020). See Appendix D for more details on the calibration (Table 1), the model equations, and computations.

12 We assume that in steady state the utility functions of recovered and susceptible individuals are the same. Recovered individuals do not modify their social activity since they become immune.

13 We set the former to 0.0062, which is the intermediate infection probability of two baseline scenarios in Hall et al. (2020). We translate in the model's units the estimates by Hall et al. (2020) of the value of each remaining year of life, \$270,000, and the average remaining life expectancy of COVID-19 victims of 14.5 years, translated to the model units. The VSL is obtained from the fraction of consumption that an agent is willing to pay to avoid a certain death risk. A more detailed description of the calculations can be found in Farboodi et al. (2021).

14 For example, Farboodi et al. (2021) choose a recovery rate of 1/7 and Dasaratha (2022) a rate of 1/14.

15 See Burki (2021)'s estimate for the original strain of SARS-CoV-2.

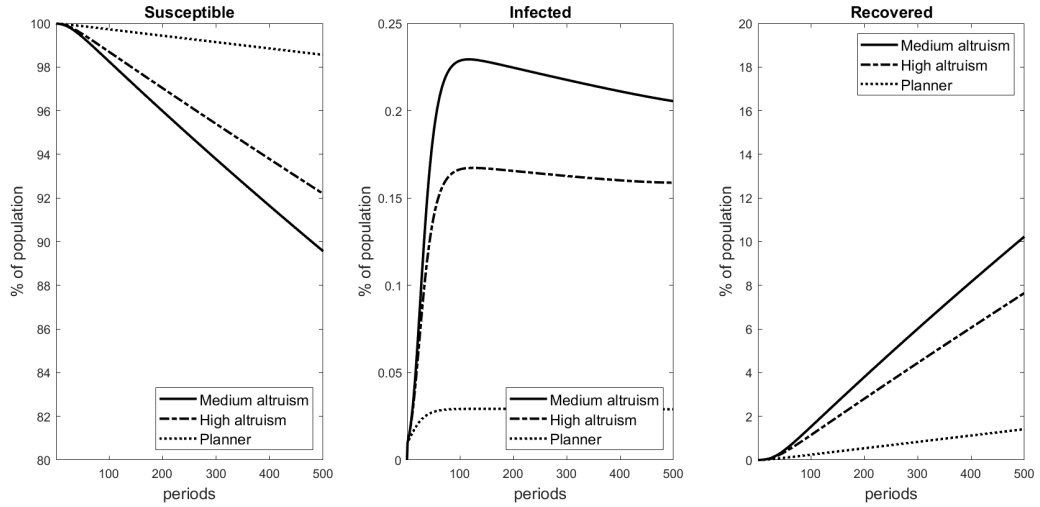

Figure 1
Comparison of the Decentralized Equilibrium with Different Degrees of Altruism and the Social Planner's Solution

Baseline model with altruism. Behavioral responses to infection risk play a fundamental role in determining the dynamic of a pandemic. When we compare the dynamics of the total shares of susceptible, infected, and recovered individuals in our baseline (homogeneous SIR) model with endogenous social activity to the traditional SIR model with exogenous contact rates, we find that the peak of the infection curve is significantly flattened in the model with endogenous social activity.[16] Susceptible agents internalize the consequences of the infection risk for their future utility and reduce their level of social activity. Due to this more careful behavior, the infection probability in our model drops.

Figure 1 demonstrates the role of altruism in flattening the curve further by reducing the total share of infected individuals. We set δ to 0.5 and 1, representing medium and high degrees of altruism, respectively. The more altruistic infected individuals are the more they reduce their social activity, lowering the infection probability which, in turn, leads to a lower share of infected individuals.

The different levels of social activity depending on the degree of altruism are displayed in Figure 2. When infected individuals are not altruistic at all (left panel), they do not alter their behavior in response to the pandemic. However, when they exhibit a high—in fact, maximum—degree of altruism ($\delta = 1$, second rightmost panel), they reduce their

16 See Figure 5 in Appendix C. In the traditional model, social activity is set equal to the average steady-state level of social activity, i.e., 1. The other parameters are the same across the two models.

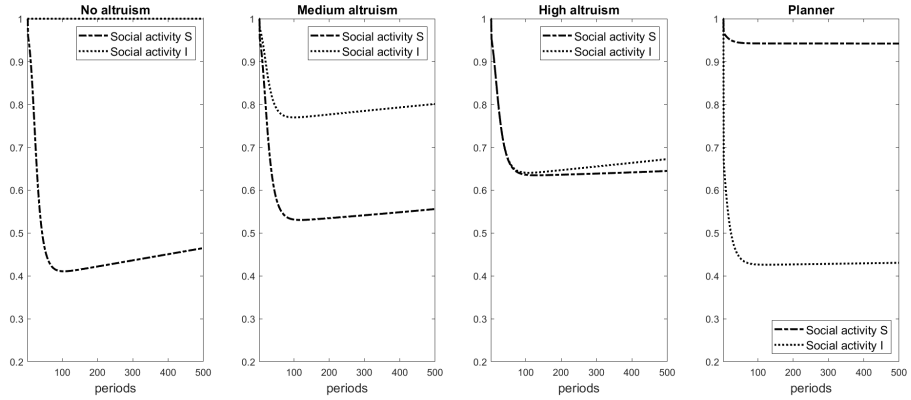

Figure 2
Comparison of Social Activity of Susceptible (S) and Infected (I) Individuals in the Decentralized Equilibrium with Different Degrees of Altruism and the Social Planner's Solution

social activity on impact in response to the infection shock by roughly the same amount as susceptible individuals do.[17] Consistent with Proposition 1, Figure 2 shows as well that when the degree of altruism increases, susceptible individuals reduce their social contacts by less since infected individuals carry part of the burden by internalizing some of the infection risk.

Social planner vs. decentralized equilibrium. Our results may lead one to believe that a society with the maximum degree of altruism may not need any planning intervention. This is, however, not the case. As can be seen in Figure 1 (two leftmost panels), the number of infected individuals is lower but the number of susceptible individuals is higher in the social planner's solution than in the decentralized solution with the maximum degree of altruism ($\delta = 1$). As the rightmost panel of Figure 2 shows, this is consistent with the fact that the social planner reduces the level of social activity of infected individuals significantly more in comparison to the decentralized equilibrium, illustrating Proposition 2. This, in turn, allows susceptible agents to reduce their social contacts by less compared to the decentralized equilibrium.

To explain why this is the case, we consider the two types of inefficiencies described in Corollary 3. First, the presence of altruism reduces the extent of the static inefficiency, but

17 Note that as the pandemic progresses, the social activity of infected individuals exceeds that of susceptible individuals, as the former take into account the population share of susceptible individuals, which is decreasing over time.

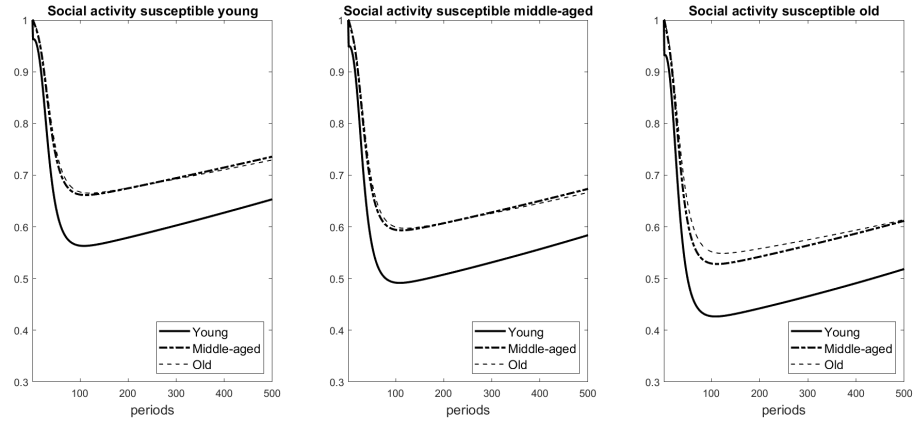

(a) Social Activity of Susceptible Individuals

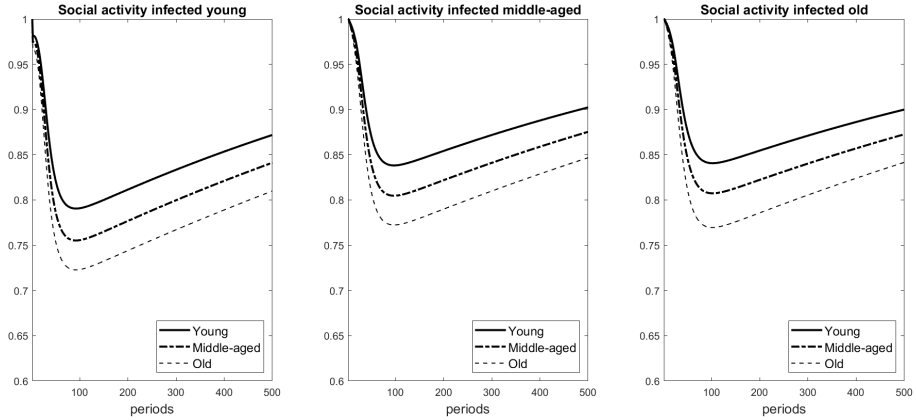

(b) Social Activity of Infected Individuals

Figure 3
Differentiated Social Activity of Susceptible (panel a) and Infected (panel b) Young, Middle-aged, and Old Individuals in the Endogenous Network Model ($\delta = 0.5$).

only up to the degree of congestion given by the geography, i.e., the returns to scale of the matching function. Second, and more importantly, altruism does not reduce the extent of the dynamic inefficiency. The existence of a dynamic inefficiency constitutes a crucial difference in comparison to other models. Farboodi et al. (2021), for instance, discuss a fully altruistic equilibrium, which in their case can coincide with the social planner's allocation. In our model, this is not the case due to dynamic considerations. The planner internalizes the risk of infection not only at time t but also in all future periods (as highlighted in a different context also by Moser and Yared, 2022).

Endogenous network model. We now simulate the model with heterogeneous agents which belong to different age groups with different recovery rates. The social intensity of

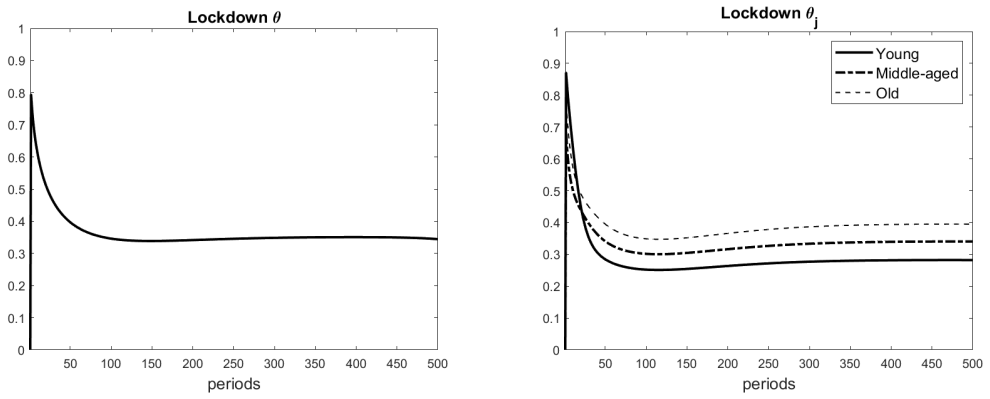

(a) Baseline model **(b) Network model**

Figure 4
Optimal Lockdown in the Baseline and the Endogenous Network Model ($\delta = 0.5$)

agents of each group vis-à-vis their own and each other group is chosen endogenously. We assume that the infection shock occurs in the group of young agents, and we set the degree of altruism to $\delta = 0.5$.

Figure 3a shows the social-activity intensities of susceptible young, middle-aged, and old agents vis-à-vis the three different groups relative to their steady-state levels. Susceptible old agents reduce their overall social activity the most due to their lower recovery rates. Susceptible young agents, in turn, reduce their social activity the least and have, therefore, the highest infection probability, as Figure 7 in Appendix C shows. In line with Corollary 1, all three groups primarily reduce their contact exposure to young agents (solid line), as the latter are in the group with the highest share of infected agents and therefore the most significant spreaders.[18] Figure 3b illustrates Corollary 2: even for a medium degree of altruism, infected agents reduce their social activity the most vis-à-vis the most vulnerable group with the lowest recovery rate, namely the old agents.

Figure 8 in Appendix C presents the aggregate levels of social-activity intensity of all three susceptible age groups for two different degrees of altruism ($\delta = 0.5$ vs. 1). All—and especially old—susceptible agents reduce their social activity by less when infected individuals are more altruistic (see left vs. right panel). This is again driven by the fact that—especially young—infected agents that are more altruistic reduce their activity by more as a higher degree of altruism makes them more cautious, as Figure 9 in Appendix C showcases.

18 Figure 6 in Appendix C displays the course of the pandemic separately for the three age groups with endogenous vs. exogenous contact rates.

Optimal lockdown policy. We conclude our analysis by quantifying in Figure 4 the optimal lockdown policy, θ, chosen by the Ramsey planner for both the baseline (left panel) and the endogenous network model (right panel). The Ramsey planner sets a very strict lockdown at the beginning of the pandemic so as to cut the share of infected agents immediately to a bearable level, and then relaxes stringency measures accordingly.

In the endogenous network model, lockdown policies are set differentially across age groups. On impact, the planner optimally restricts social interactions in the young age group the most, as these are the agents with the highest infection numbers. After this immediate reaction, lockdowns are strictest for the old age group since the disease is most dangerous for its members.

4. Conclusion

We derive and simulate an epidemiological model in which agents optimally choose the degree of social activity, while internalizing the risk of infection for themselves and for others in the presence of altruistic preferences. We also develop a network variant of this model with heterogeneous agents that differ in their recovery rates. By affecting both infected and susceptible individuals' behavior, altruism can contribute to flattening the infection curve. However, we show that even in the presence of a maximum degree of altruism, non-negligible health externalities remain. To address them, a social planner would choose a sharp lockdown for all on impact before restricting social activities primarily for vulnerable groups. Our model can be easily extended to include other dimensions of heterogeneity, add uncertainty, or study different policy interventions, which we leave for future research.

References

Acemoglu, D., Chernozhukov, V., Werning, I., and Whinston, M. D. (2021). Optimal Targeted Lockdowns in a Multigroup SIR Model. *American Economic Review: Insights*, 3(4):487–502.

Alfaro, L., Faia, E., Lamersdorf, N., and Saidi, F. (2022). Health Externalities and Policy: The Role of Social Preferences. *Management Science*, 68(9):6355–7064.

Andreoni, J. (1989). Giving with Impure Altruism: Applications to Charity and Ricardian Equivalence. *Journal of Political Economy*, 97(6):1447–1458.

Andreoni, J. (1993). An Experimental Test of the Public-Goods Crowding-Out Hypothesis. *American Economic Review*, 83(5):1317–1327.

Andreoni, J. and Miller, J. (2002). Giving according to GARP: An Experimental Test of the Consistency of Preferences for Altruism. *Econometrica*, 70(2):737–753.

Becker, G. S. (1974). A Theory of Social Interactions. *Journal of Political Economy*, 82(6):1063–1093.

Bolton, G. E. and Ockenfels, A. (2000). ERC: A Theory of Equity, Reciprocity, and Competition. *American Economic Review*, 90(1):166–193.

Brock, W. A. and Durlauf, S. N. (2001). Discrete Choice with Social Interactions. *Review of Economic Studies*, 68(2):235–260.

Brotherhood, L., Cavalcanti, T., Da Mata, D., and Santos, C. (2022). Slums and Pandemics. *Journal of Development Economics*, 157:102882.

Brotherhood, L., Kircher, P., Santos, C., and Tertilt, M. (2020). An Economic Model of the Covid-19 Pandemic with Young and Old Agents: Behavior, Testing and Policies. *CEPR Discussion Paper No. 14695*.

Burki, T. K. (2021). Omicron Variant and Booster COVID-19 Vaccines. *The Lancet Respiratory Medicine*, 10(2).

Cabrales, A., Calvó-Armengol, A., and Zenou, Y. (2011). Social Interactions and Spillovers. *Games and Economic Behavior*, 72(2):339–360.

Case, A. C. and Katz, L. F. (1991). The Company You Keep: The Effects of Family and Neighborhood on Disadvantaged Youths. *NBER Working Paper No. 3705*.

Chakrabarti, S., Krasikov, I., and Lamba, R. (2022). Behavioral Epidemiology: An Economic Model to Evaluate Optimal Policy in the Midst of a Pandemic. *Penn State University Working Paper*.

Currarini, S., Jackson, M. O., and Pin, P. (2009). An Economic Model of Friendship: Homophily, Minorities, and Segregation. *Econometrica*, 77(4):1003–1045.

Dasaratha, K. (2022). Virus Dynamics with Behavioral Responses. *Yale University Working Paper*.

Diamond, P. A. (1982). Aggregate Demand Management in Search Equilibrium. *Journal of Political Economy*, 90(5):881–894.

Doepke, M. and Tertilt, M. (2009). Women's Liberation: What's in It for Men? *Quarterly Journal of Economics*, 124(4):1541–1591.

Duffie, D., Gârleanu, N., and Pedersen, L. H. (2005). Over-the-Counter Markets. *Econometrica*, 73(6):1815–1847.

Falk, A., Becker, A., Dohmen, T., Enke, B., Huffman, D., and Sunde, U. (2018). Global Evidence on Economic Preferences. *Quarterly Journal of Economics*, 133(4):1645–1692.

Farboodi, M., Jarosch, G., and Shimer, R. (2021). Internal and External Effects of Social Distancing in a Pandemic. *Journal of Economic Theory*, 196:105293.

Farboodi, M., Jarosch, G., and Shimer, R. (2023). The Emergence of Market Structure. *Review of Economic Studies*, 90(1):261–292.

Fehr, E. and Gächter, S. (2000). Fairness and Retaliation: The Economics of Reciprocity. *Journal of Economic Perspectives*, 14(3):159–181.

Fehr, E. and Schmidt, K. M. (1999). A Theory of Fairness, Competition, and Cooperation. *Quarterly Journal of Economics*, 114(3):817–868.

Fenichel, E. P. (2013). Economic Considerations for Social Distancing and Behavioral Based Policies during an Epidemic. *Journal of Health Economics*, 32(2):440–451.

Fenichel, E. P., Castillo-Chavez, C., Ceddia, M. G., Chowell, G., Parra, P. A. G., Hickling, G. J., Holloway, G., Horan, R., Morin, B., Perrings, C., Springborn, M., Velazquez, L., and Villalobos, C. (2011). Adaptive Human Behavior in Epidemiological Models. *Proceedings of the National Academy of Sciences*, 108:6306–6311.

Frey, B. S. and Meier, S. (2004). Pro-social Behavior in a Natural Setting. *Journal of Economic Behavior & Organization*, 54(1):65–88.

Garibaldi, P., Moen, E. R., and Pissarides, C. A. (2020a). Modelling Contacts and Transitions in the SIR Epidemics Model. *Covid Economics: Vetted and Real-Time Papers*, 5.

Garibaldi, P., Moen, E. R., and Pissarides, C. A. (2020b). Static and Dynamic Inefficiencies in an Optimizing Model of Epidemics. *CEPR Discussion Paper No. 15439*.

Glaeser, E. L., Sacerdote, B., and Scheinkman, J. A. (1996). Crime and Social Interactions. *Quarterly Journal of Economics*, 111(2):507–548.

Greenwood, J., Kircher, P., Santos, C., and Tertilt, M. (2019). An Equilibrium Model of the African HIV/AIDS Epidemic. *Econometrica*, 87(4):1081–1113.

Hall, R. E., Jones, C. I., and Klenow, P. J. (2020). Trading off Consumption and COVID-19 Deaths. *Minneapolis Fed Quarterly Review*, 42(1).

Hethcote, H. W. (2000). The Mathematics of Infectious Diseases. *SIAM Review*, 42(4):599–653.

Hofstede, G. (2001). *Culture's Consequences: Comparing Values, Behaviors, Institutions and Organizations across Nations*. Sage Publications.

Keeling, M. J. and Eames, K. T. (2005). Networks and Epidemic Models. *Journal of The Royal Society Interface*, 2(4):295–307.

Kermack, W. O. and McKendrick, A. G. (1927). A Contribution to the Mathematical Theory of Epidemics. *Proceedings of the Royal Society of London*, 115(772):700–721.

Kiss, I. Z., Miller, J. C., Simon, P. L., et al. (2017). *Mathematics of Epidemics on Networks*.

Kremer, M. (1996). Integrating Behavioral Choice into Epidemiological Models of AIDS. *Quarterly Journal of Economics*, 111(2):549–573.

Makris, M. (2021). Covid and Social Distancing with a Heterogenous Population. *Economic Theory*.

Moinet, A., Pastor-Satorras, R., and Barrat, A. (2018). Effect of Risk Perception on Epidemic Spreading in Temporal Networks. *Physical Review E*, 97:012313.

Moser, C. and Yared, P. (2022). Pandemic Lockdown: The Role of Government Commitment. *Review of Economic Dynamics*, 46:27–50.

Newman, M. (2018). *Networks*. Oxford University Press, 2nd edition.

Pastor-Satorras, R. and Vespignani, A. (2001a). Epidemic Dynamics and Endemic States in Complex Networks. *Physical Review E*, 63(6):066117.

Pastor-Satorras, R. and Vespignani, A. (2001b). Epidemic Spreading in Scale-Free Networks. *Physical Review Letters*, 86(14):3200–3203.

Perra, N., Gonçalves, B., Pastor-Satorras, R., and Vespignani, A. (2012). Activity Driven Modeling of Time Varying Networks. *Scientific Reports*, 2(469).

Pissarides, C. A. (2000). *Equilibrium Unemployment Theory*. The MIT Press, 2nd edition.

Rachel, L. (2022). An Analytical Model of Behavior and Policy in an Epidemic. *UCL Working Paper*.

Rubinstein, A. and Wolinsky, A. (1987). Middlemen. *Quarterly Journal of Economics*, 102(3):581–593.

Spolaore, E. and Wacziarg, R. (2013). How Deep are the Roots of Economic Development? *Journal of Economic Literature*, 51(2):325–369.

Talamàs, E. and Vohra, R. (2020). Free and Perfectly Safe but only Partially Effective Vaccines Can Harm Everyone. *Games and Economic Behavior*, 122:277–289.

Toxvaerd, F. (2019). Rational Disinhibition and Externalities in Prevention. *International Economic Review*, 60(4):1737–1755.

Toxvaerd, F. (2021). Contacts, Altruism and Competing Externalities. *CEPR Discussion Paper No. 15903*.

Wu, L. and Shimer, R. (2021). Diffusion on a Sorted Network. *University of Chicago Working Paper*.

A. Proofs

A.1. Proof of Proposition 1

The first-order condition for infected individuals who exhibit a non-zero degree of altruism is $\frac{\partial U(x^I_{s,t})}{\partial x^I_{s,t}} + \delta S_t \beta \frac{\partial p_t(\cdot)}{\partial x^I_{s,t}}(V^I_{t+1} - V^S_{t+1}) = 0$. If they do not exhibit any altruism, i.e., $\delta = 0$, it becomes $\frac{\partial U(x^I_{s,t})}{\partial x^I_{s,t}} = 0$. Since $V^I_{t+1} - V^S_{t+1} < 0$, the term $\frac{\partial U(x^I_{s,t})}{\partial x^I_{s,t}}$ has to be larger in the presence of altruism ($\delta > 0$) and, thus, the $x^I_{s,t}$ that solves the first equation with altruism is smaller. The larger the degree of altruism δ, the larger the marginal utility, $\frac{\partial U(x^I_{s,t})}{\partial x^I_{s,t}}$, and, thus, the smaller $x^I_{s,t}$.

From the first-order condition for the susceptible individuals, (5), it follows that $\frac{\partial U(x^S_{s,t})}{\partial x^S_{s,t}} = \beta \frac{\partial p_t(\cdot)}{\partial x^S_{s,t}}(V^S_{t+1} - V^I_{t+1}) = \beta \eta x^I_{s,t}(\overline{x}_{s,t})^{\alpha-1} I_t (V^S_{t+1} - V^I_{t+1})$. Given the states, if $x^I_{s,t}$ is lower when infected individuals exhibit altruism, it follows that $\frac{\partial U(x^S_{s,t})}{\partial x^S_{s,t}}$ is lower as well, implying a larger $x^S_{s,t}$. The lower $x^I_{s,t}$, the lower $\frac{\partial U(x^S_{s,t})}{\partial x^S_{s,t}}$ and, thus, the larger $x^S_{s,t}$.

A.2. Proof of Proposition 2

We compare the first-order conditions for social activities of infected individuals in the decentralized and the social planner's equilibrium, namely (6) and (12).[19] To prove that the social activity of infected agents chosen by the social planner is lower than in the decentralized equilibrium, we show that

$$\beta \left[\frac{S_t}{I_t} \frac{\partial p^P_t(\cdot)}{\partial x^I_{s,t}} - \delta S_t \frac{\partial p_t}{\partial x^I_{s,t}} \right] (\hat{V}^I_{t+1} - \hat{V}^S_{t+1}) + \beta \frac{S_t}{I_t}(1 - p^P_t(\cdot)) \left(\frac{\partial \hat{V}^S_{t+1}}{\partial S_{t+1}} \frac{\partial S_{t+1}}{\partial x^I_{s,t}} + \frac{\partial \hat{V}^S_{t+1}}{\partial I_{t+1}} \frac{\partial I_{t+1}}{\partial x^I_{s,t}} \right) < 0, \tag{20}$$

Only if the inequality in (20) holds, the social planner chooses a higher marginal utility and, hence, a lower level of social activity of infected individuals.

19 Note that we compare the decentralized equilibrium with any degree of altruism to the social planner's equilibrium without altruism. We set $\delta = 0$ in the latter since in the presence of a central social planner, infected agents know that the planner takes into account all the externalities, which is why there is no particular role for altruism in that instance. However, one can show that our results would continue to hold if $\delta > 0$ also in the social planner's equilibrium.

We first examine the second term of (20). Note that:

$$\frac{\partial \hat{V}^S_{t+1}}{\partial S_{t+1}}\frac{\partial S_{t+1}}{\partial x^I_{s,t}} + \frac{\partial \hat{V}^S_{t+1}}{\partial I_{t+1}}\frac{\partial I_{t+1}}{\partial x^I_{s,t}} = \left(-\frac{\partial \hat{V}^S_{t+1}}{\partial S_{t+1}} + \frac{\partial \hat{V}^S_{t+1}}{\partial I_{t+1}}\right)\frac{\partial p^P_t(\cdot)}{\partial x^I_{s,t}} S_t \tag{21}$$

$$= \beta(\hat{V}^I_{t+2} - \hat{V}^S_{t+2})\left[-\frac{\partial p^P_{t+1}(\cdot)}{\partial S_{t+1}} + \frac{\partial p^P_{t+1}(\cdot)}{\partial I_{t+1}}\right]\frac{\partial p^P_t(\cdot)}{\partial x^I_{s,t}} S_t. \tag{22}$$

Note further that:

$$\begin{aligned}-\frac{\partial p^P_{t+1}(\cdot)}{\partial S_{t+1}} + \frac{\partial p^P_{t+1}(\cdot)}{\partial I_{t+1}} =& -(\alpha-1)\eta x^S_{s,t+1} x^I_{s,t+1}(\overline{x}_{s,t+1})^{\alpha-2} I_{t+1} x^S_{s,t+1} + \\ &+ (\alpha-1)\eta x^S_{s,t+1} x^I_{s,t+1}(\overline{x}_{s,t+1})^{\alpha-2} I_{t+1} x^I_{s,t+1} + \eta x^S_{s,t+1} x^I_{s,t+1}(\overline{x}_{s,t+1})^{\alpha-1}.\end{aligned} \tag{23}$$

Under $\alpha = 1$, implying a quadratic matching function, this last expression, (23), is positive.[20] Therefore, the second term in (20) is negative only if $\hat{V}^I_{t+2} - \hat{V}^S_{t+2} < 0$ (Assumption 1) and $S_t > 0$, since $\frac{\partial p^P_t(\cdot)}{\partial x^I_{s,t}} > 0$ and $p^P_t(\cdot) < 1$.

The first part of (20) is negative as well only if $\hat{V}^I_{t+1} - \hat{V}^S_{t+1} < 0$ and $\frac{S_t}{I_t}\frac{\partial p^P_t(\cdot)}{\partial x^I_{s,t}} > \delta S_t \frac{\partial p_t}{\partial x^I_{s,t}}$. With $\alpha = 1$, we can write the latter condition as: $\frac{S_t}{I_t}\eta x^S_{s,t} I_t > \delta S_t \eta x^S_{s,t} I_t$. The inequality holds for any δ, only if the share of susceptible agents is positive, $S_t > 0$, implying $I_t < 1$.

To sum up, only if the whole expression in (20) is negative, the marginal utility of social interactions of infected individuals chosen by the social planner is larger than the one under the decentralized equilibrium, which means that the level of social activities of infected individuals, $x^I_{s,t}$, chosen by the social planner is smaller.

A.3. Proof of Proposition 3

To compare the solutions of the decentralized and the social planner's equilibrium in the endogenous network variant of our model, we again compare the first-order conditions for social activities of infected individuals of group j vis-à-vis group k, $x^{I,jk}_{s,t}$, namely (8) and

20 It would also be positive for different values of α if the total share of infected agents, I_{t+1}, is close to zero.

(31). As before, the social planner chooses a lower level for the social activity of infected individuals in group j vis-à-vis group k only if

$$\frac{1}{I_t^j}\sum_n S_t^n \beta \frac{\partial p_t^{Pn}(\cdot)}{\partial x_{s,t}^{I,jk}}(\hat{V}_{t+1}^{I,n} - \hat{V}_{t+1}^{S,n}) - \delta \frac{S_t^k}{N_t^k}\beta \frac{\partial p_t^k(\cdot)}{\partial x_{s,t}^{I,jk}}(V_{t+1}^{I,k} - V_{t+1}^{S,k})$$
$$+\frac{1}{I_t^j}\sum_n S_t^n \beta (1 - p_t^{Pn}(\cdot)) \sum_m \left(\frac{\partial \hat{V}_{t+1}^{S,n}}{\partial S_{t+1}^m}\frac{\partial S_{t+1}^m}{\partial x_{s,t}^{I,jk}} + \frac{\partial \hat{V}_{t+1}^{S,n}}{\partial I_{t+1}^m}\frac{\partial I_{t+1}^m}{\partial x_{s,t}^{I,jk}} \right) < 0, \tag{24}$$

where p_t^{Pn} is given by equation (18) and (the summations over) n and m refer to all groups, including j and k.

We proceed as in the proof for Proposition 2 and argue that only if the inequality (24) holds, the social planner chooses a higher marginal utility and, hence, a lower level of social activity. As before, under the assumption of a quadratic matching function, i.e., $\alpha = 1$, the last term on the left-hand side of (24) is negative for all groups n only if $\hat{V}_{t+2}^{I,n} - \hat{V}_{t+2}^{S,n} < 0$.

To show that the remaining expression is negative as well, we show that $\frac{1}{I_t^j}\sum_n S_t^n \beta \frac{\partial p_t^{Pn}(\cdot)}{\partial x_{s,t}^{I,jk}}(\hat{V}_{t+1}^{I,n} - \hat{V}_{t+1}^{S,n}) - \delta \frac{S_t^k}{N_t^k}\beta \frac{\partial p_t^k(\cdot)}{\partial x_{s,t}^{I,jk}}(V_{t+1}^{I,k} - V_{t+1}^{S,k}) < 0$. Due to our assumptions for the matching function and $\alpha = 1$, this becomes $\beta \left[\frac{1}{I_t^j} S_t^k \frac{\partial p_t^{Pk}(\cdot)}{\partial x_{s,t}^{I,jk}} - \delta \frac{S_t^k}{N_t^k}\frac{\partial p_t^k(\cdot)}{\partial x_{s,t}^{I,jk}} \right](\hat{V}_{t+1}^{I,k} - \hat{V}_{t+1}^{S,k}) < 0$. According to Assumption 1, $(V_{t+1}^{I,k} - V_{t+1}^{S,k}) < 0$, therefore, this inequality holds only if $\frac{S_t^k}{I_t^j}\eta x_{s,t}^{S,kj} I_t^j > \delta \frac{S_t^k}{N_t^k}\eta x_{s,t}^{S,kj} I_t^j$, which is the case if $\delta I_t^j < N_t^k$. Hence, if the number of infected agents in group j multiplied by their level of altruism is smaller than the total population in group k, the social planner reduces the level of social activity of infected agents of group j vis-à-vis group k by more compared to the decentralized equilibrium.

A.4. Proof of Proposition 4

We start by obtaining the ratio of the marginal utility from the social activity for an infected agent and the marginal utility from the social activity for a susceptible agent, which we dub

the marginal rate of substitution between one infected and one susceptible agent, in the decentralized economy (DE) at time t (in the case with maximum altruism, $\delta = 1$):

$$MRS^{DE}_{t,I,S} = \frac{\frac{\partial U(x^I_{s,t})}{\partial x^I_{s,t}}}{\frac{\partial U(x^S_{s,t})}{\partial x^S_{s,t}}} = \frac{\frac{\partial p_t}{\partial x^I_{s,t}}}{\frac{\partial p_t}{\partial x^S_{s,t}}}. \tag{25}$$

The respective marginal rate of substitution in the social planner's (SP) solution is:

$$MRS^{SP}_{t,I,S} = \frac{\frac{\partial p^P_t}{\partial x^I_{s,t}}(V^I_{t+1} - V^S_{t+1}) + (1 - p^P_t)\Psi^I_t}{\frac{\partial p^P_t}{\partial x^S_{s,t}}(V^I_{t+1} - V^S_{t+1}) + (1 - p^P_t)\Psi^S_t}, \tag{26}$$

where

$$\Psi^S_t = \frac{\partial \hat{V}^S_{t+1}}{\partial S_{t+1}}\frac{\partial S_{t+1}}{\partial x^S_{s,t}} + \frac{\partial \hat{V}^S_{t+1}}{\partial I_{t+1}}\frac{\partial I_{t+1}}{\partial x^S_{s,t}} \tag{27}$$

$$\Psi^I_t = \frac{\partial \hat{V}^S_{t+1}}{\partial S_{t+1}}\frac{\partial S_{t+1}}{\partial x^I_{s,t}} + \frac{\partial \hat{V}^S_{t+1}}{\partial I_{t+1}}\frac{\partial I_{t+1}}{\partial x^I_{s,t}}. \tag{28}$$

Note that $-\frac{\partial S_{t+1}}{\partial x^S_{s,t}} = \frac{\partial I_{t+1}}{\partial x^S_{s,t}} = \frac{\partial p^P_t}{\partial x^S_{s,t}} S_t$ and $-\frac{\partial S_{t+1}}{\partial x^I_{s,t}} = \frac{\partial I_{t+1}}{\partial x^I_{s,t}} = \frac{\partial p^P_t}{\partial x^I_{s,t}} S_t$, so (26) becomes:

$$MRS^{SP}_{t,I,S} = \frac{\frac{\partial p^P_t}{\partial x^I_{s,t}}[V^I_{t+1} - V^S_{t+1} + (1 - p^P_t)(-\frac{\partial \hat{V}^S_{t+1}}{\partial S_{t+1}}S_t + \frac{\partial \hat{V}^S_{t+1}}{\partial I_{t+1}}S_t)]}{\frac{\partial p^P_t}{\partial x^S_{s,t}}[V^I_{t+1} - V^S_{t+1} + (1 - p^P_t)(-\frac{\partial \hat{V}^S_{t+1}}{\partial S_{t+1}}S_t + \frac{\partial \hat{V}^S_{t+1}}{\partial I_{t+1}}S_t)]} = \frac{\frac{\partial p^P_t}{\partial x^I_{s,t}}}{\frac{\partial p^P_t}{\partial x^S_{s,t}}}. \tag{29}$$

Under a lockdown policy that sets $p_t = p^P_t$, it follows that the marginal rate of substitution in (29) is equal to the one in (25).

B. First-Order Conditions of the Social Planner in the SIR-Network Model with Endogenous Cross-Links

The first-order conditions for the social planner's problem of the SIR-network model for recovered individuals' social activities are equivalent to those obtained under the decentralized

equilibrium. For the levels of social activity of susceptible and infected individuals in each group j vis-à-vis each group k, $x_{s,t}^{S,jk}$ and $x_{s,t}^{I,jk}$, the first-order conditions are as follows:

$$S_t^j \frac{\partial U(x_{s,t}^{S,j})}{\partial x_{s,t}^{S,jk}} + \sum_n S_t^n \left\{ \beta \frac{\partial p^{Pn}(\cdot)}{\partial x_{s,t}^{S,jk}} (\hat{V}_{t+1}^{I,n} - \hat{V}_{t+1}^{S,n}) + \beta(1 - p_t^{Pn}(\cdot)) \sum_m \left[\frac{\partial \hat{V}_{t+1}^{S,n}}{\partial S_{t+1}^m} \frac{\partial S_{t+1}^m}{\partial x_{s,t}^{S,jk}} + \frac{\partial \hat{V}_{t+1}^{S,n}}{\partial I_{t+1}^m} \frac{\partial I_{t+1}^m}{\partial x_{s,t}^{S,jk}} \right] \right\} = 0 \tag{30}$$

$$I_t^j \frac{\partial U(x_{s,t}^{I,j})}{\partial x_{s,t}^{I,jk}} + \sum_n S_t^n \left\{ \beta \frac{\partial p^{Pn}(\cdot)}{\partial x_{s,t}^{I,jk}} (\hat{V}_{t+1}^{I,n} - \hat{V}_{t+1}^{S,n}) + \beta(1 - p_t^{Pn}(\cdot)) \sum_m \left[\frac{\partial \hat{V}_{t+1}^{S,n}}{\partial S_{t+1}^m} \frac{\partial S_{t+1}^m}{\partial x_{s,t}^{I,jk}} + \frac{\partial \hat{V}_{t+1}^{S,n}}{\partial I_{t+1}^m} \frac{\partial I_{t+1}^m}{\partial x_{s,t}^{I,jk}} \right] \right\} = 0, \tag{31}$$

where p_t^{Pn} is given by equation (18) and (the summations over) n and m refer to all groups, including j and k.

C. Additional Figures

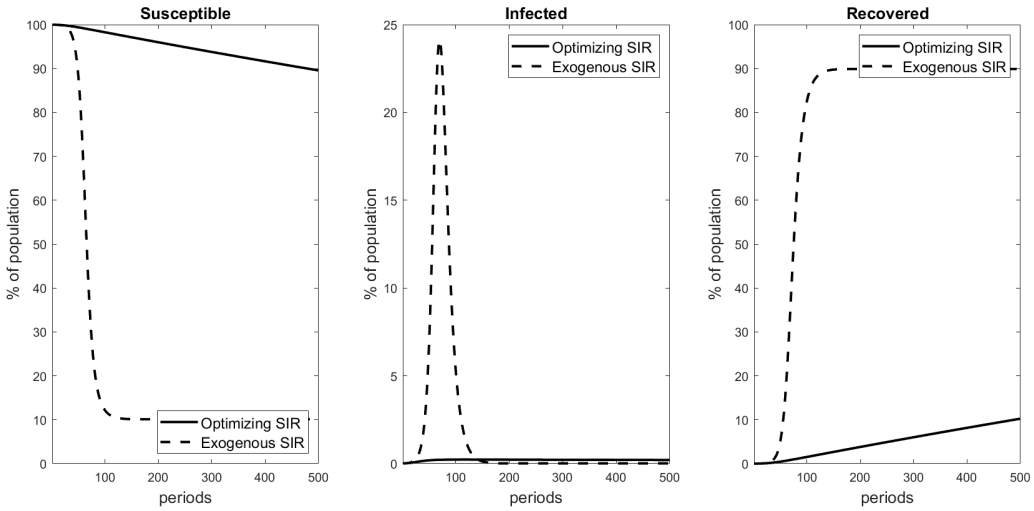

Figure 5
Comparison of the Homogeneous SIR Model with Endogenous Social Activity ($\delta = 0.5$) and the Traditional SIR Model with Constant Exogenous Contact Rates

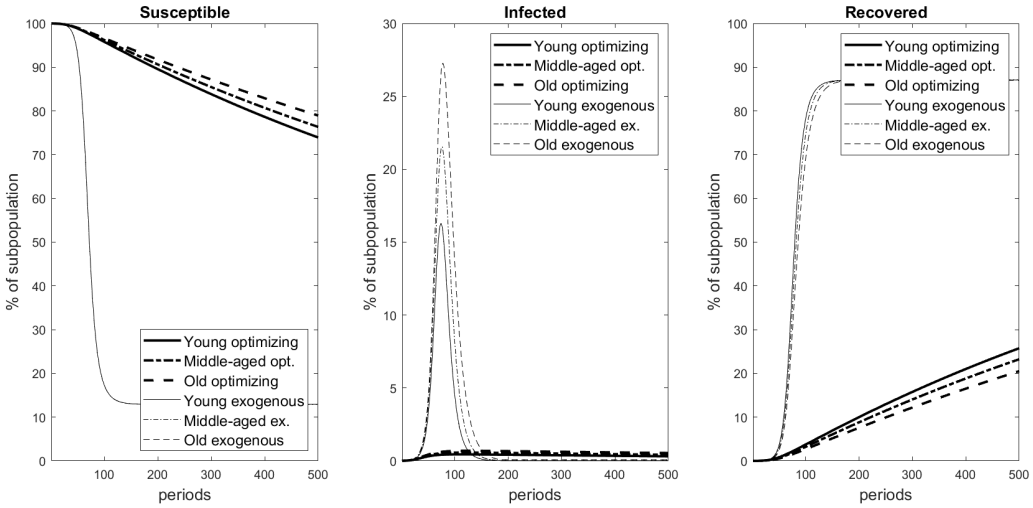

Figure 6
Comparison of SIR-Network Models with Endogenous Social Activity ($\delta = 0.5$) vs. Constant Exogenous Contact Rates

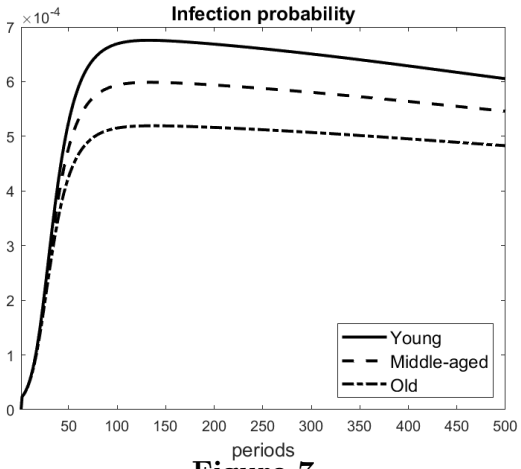

Figure 7
Dynamics of Infection Probabilities in the SIR-Network Model ($\delta = 0.5$)

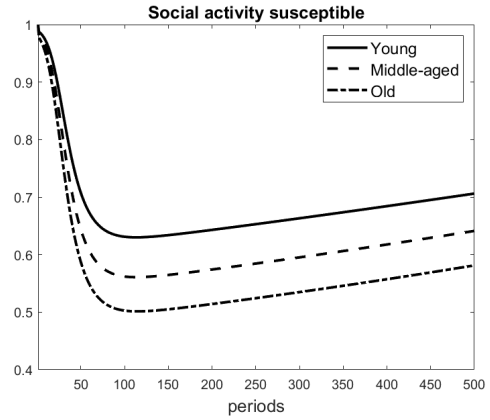

(a) $\delta = 0.5$

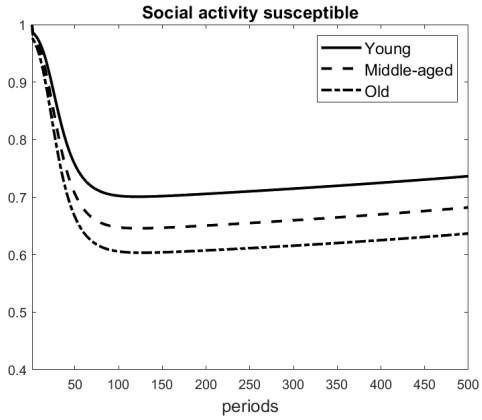

(b) $\delta = 1$

Figure 8
Aggregate Social Activity of Susceptible Young, Middle-aged, and Old Individuals with Different Degrees of Altruism in the SIR-Network Model

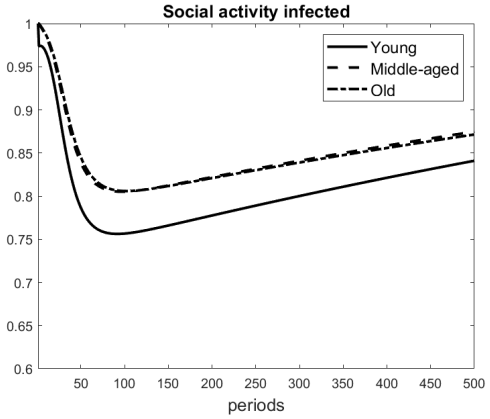

(a) $\delta = 0.5$

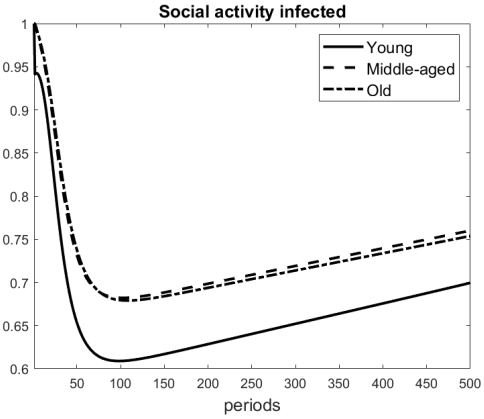

(b) $\delta = 1$

Figure 9
Aggregate Social Activity of Infected Young, Middle-aged, and Old Individuals with Different Degrees of Altruism in the SIR-Network Model

D. Details for the Simulations

An overview of the parameter values can be found in Table 1.

Table 1
Calibration

Parameter	Value	Description
α	1	Matching function's returns to scale
$c_S = c_I$	1	Steady-state social activity
γ	1/10	Recovery rate
η	2.5*γ	Transmission rate
C_I	197	Cost of infection
δ	[0,1]	Degree of altruism
β	0.99	Discount factor
ϵ	0.0001	Initial infection shock of 0.01%
γ_y	1/7	Recovery rate young
γ_m	1/10	Recovery rate middle-aged
γ_o	1/14	Recovery rate old
N_y	0.53	Population share young
N_m	0.26	Population share middle-aged
N_o	0.21	Population share old

The model equations of the baseline model that we use for the simulations are as follows:

$$S_{t+1} = S_t - p_t S_t - \epsilon \mathbb{1}_{t=1} \tag{A1}$$

$$I_{t+1} = I_t + p_t S_t - \gamma I_t + \epsilon \mathbb{1}_{t=1} \tag{A2}$$

$$R_{t+1} = R_t + \gamma I_t \tag{A3}$$

$$V_t^S = U(x_{s,t}^S) + \beta[p_t V_{t+1}^I + (1-p_t) V_{t+1}^S] \tag{A4}$$

$$V_t^I = U(x_{s,t}^I) - C_t^I + \beta[(1-\gamma) V_{t+1}^I + \gamma V_{t+1}^R] + \delta S_t V_t^S \tag{A5}$$

$$V_t^R = U(x_{s,t}^R) + \beta V_{t+1}^R \tag{A6}$$

$$p_t(\cdot) = \eta x_{s,t}^S x_{s,t}^I (\bar{x}_{s,t})^{\alpha-1} I_t \tag{A7}$$

$$\frac{\partial U(x_{s,t}^S)}{\partial x_{s,t}^S} = \beta \eta x_{s,t}^I (\bar{x}_{s,t})^{\alpha-1} I_t (V_{t+1}^S - V_{t+1}^I) \tag{A8}$$

$$\frac{\partial U(x_{s,t}^I)}{\partial x_{s,t}^I} = \delta S_t \beta \eta x_{s,t}^S (\bar{x}_{s,t})^{\alpha-1} I_t (V_{t+1}^S - V_{t+1}^I). \tag{A9}$$

Note that there is no equation for the social interactions of recovered agents, since we assume for simplicity that they are not affected by the evolution of the pandemic.

The model simulations are performed with Dynare 5.1. Initially, the economy is in a steady

state and hit by a zero-probability MIT shock, increasing the total share of infected agents from 0 to ϵ. There are no other aggregate shocks, so that we can compute a perfect-foresight solution. The default algorithm is the Newton method. Depending on the parameters and the model variant, in some cases the Newton method cannot solve the problem. In such cases, a homotopy technique is used to divide the problem into smaller steps. Specifically, the size of the shock is initially diminished, and the problems are solved iteratively, progressively increasing the shock size until the problem converges.

We use this algorithm for the simulations at hand since, first, it is a fully non-linear algorithm, allowing to account for the non-linearity that the infection probabilities bring to the SIR system. Second, our model is in discrete time, which helps to specify future variables fully, and the algorithm is well-suited for discrete-time models.

E. Limitations of the Homogeneous SIR and SIR-Network Models with Non-Optimizing Agents

In the basic homogeneous SIR model (see Kermack and McKendrick, 1927; or, more recently, Hethcote, 2000), there are three classes of agents: susceptible (S), infected (I), and recovered (R). The number of susceptible individuals decreases as they become infected. At the same time, the number of infected individuals increases by the same amount, but also declines because people recover. Recovered people are immune to the disease and, thus, stay recovered. The mathematical representation of the model is as follows:

$$S_{t+1} = S_t - \lambda I_t S_t; \quad I_{t+1} = I_t + \lambda I_t S_t - \gamma I_t; \quad R_{t+1} = R_t + \gamma I_t, \tag{A10}$$

where $N_t = S_t + I_t + R_t$ is the overall population and λ is the transmission rate of the infection.

Hence, $p_t = \lambda I_t$ is the probability that a susceptible individual becomes infected at time t. In the classical SIR model, the latter is assumed to be exogenous, constant, and homogeneous across groups. Even as agents become aware of the pandemic, it is assumed that they do not

adjust their behavior. More recent versions of the SIR model incorporate the dependence of contact rates on the heterogeneous topology of the network of contacts and mobility of people across locations (see, for example, Pastor-Satorras and Vespignani, 2001a,b). Other variants of the model incorporate the dependence of infection rates on the activity intensity of each node of the network (see Perra et al., 2012, for solving an activity-driven SIR model using mean-field theory and Moinet et al., 2018, who introduce a parameter capturing an exogenous decay of the infection risk due to precautionary behavior).

In all of these instances, however, the model's infection probability is introduced in an ad-hoc fashion and immutable over time. Overall, those relations give a naïve representation of human behavior and are, thus, subject to the Lucas critique. This is a crucial shortcoming, particularly if one intends to apply those models to optimal policy design. Indeed, assuming that agents do not change their behavior (here: their social interactions) in their best interest in response to the shocks (here: the infection shock) and to the policy itself leads to misguided policy prescriptions. Therefore, developing a sound model for the prediction of disease diffusion is ultimately crucial for the effectiveness of containment policies.

F. SIR-Network Model with Optimizing Agents and Fixed Cross-Group Contact Rates

In this section, we present a network model in which different groups choose the general level of social activity, but the cross-group contact rates are exogenous and heterogeneous. The exogenous intensity of these contacts across groups can be characterized by the degree of homophily.[21] If two groups have lower homophily and, hence, have more frequent contact with other groups, they will internalize their relative risk of infection. The groups in the community could correspond to, e.g., the age structure, different strengths in ties, or closer face-to-face interactions in the workplace. The underlying idea is that contact rates tend to be higher among peer groups.

21 It describes "the tendency of various types of individuals to associate with others who are similar to themselves" (Currarini et al., 2009). See also Fehr and Schmidt (1999) or Fehr and Gächter (2000).

Consider a population with different groups $j = 1, ..., J$. The number of people in each group is N_j. Groups have different probabilities of encounters with the other groups. The contact intensity between group j and any group k is $\xi_{j,k}$. How fast the outbreak then spreads to the rest of the network depends on the relative exposure of the initially infected group to the other groups. Each susceptible individual of group j experiences a certain number of contacts per social activity with infected individuals of her own group, but also of the other groups. The number of contacts experienced by group j depends on the average level of social activity in each group k weighted by the contact intensity across groups, and is equal to: $m^j(\hat{x}^j_{s,t}) = \left(\sum_k \xi_{j,k}(\bar{x}^{S,k}_{s,t} S^k_t + \bar{x}^{I,k}_{s,t} I^k_t + \bar{x}^{R,k}_{s,t} R^k_t)\right)^{\alpha}$.

The probability of infection of a susceptible person in group j is modified as follows: $p^j_t(\cdot) = \eta x^{S,j}_{s,t} \sum_k \left[\xi_{j,k} x^{I,k}_{s,t} \frac{m^j(\hat{x}^j_{s,t})}{\hat{x}^j_{s,t}} I^k_t\right]$, where $k = 1, .., J$ and $\xi_{j,j} = 1$. The probability of meeting an infected person from any other group k is weighted by the likelihood of the contacts across groups, $\xi_{j,k}$. As before, atomistic individuals take the average social activity and the average social encounters as given. The first-order condition for the level of social activity of susceptible individuals belonging to group j now reads as follows:

$$\frac{\partial U(x^{S,j}_{s,t})}{\partial x^{S,j}_{s,t}} + \beta\eta \sum_k \xi_{j,k} x^{I,k}_{s,t} \frac{m^j(\hat{x}^j_{s,t})}{\hat{x}^j_{s,t}} I^k_t (V^{I,j}_{t+1} - V^{S,j}_{t+1}) = 0. \tag{A11}$$

We can now derive the first-order condition for the level of social activity of infected individuals belonging to group j:

$$\frac{\partial U(x^{I,j}_{s,t})}{\partial x^{I,j}_{s,t}} + \delta\beta\eta \sum_k \frac{S^k_t}{N^k_t} \xi_{k,j} x^{S,k}_{s,t} \frac{m^k(\hat{x}^k_{s,t})}{\hat{x}^k_{s,t}} I^j_t (V^{I,k}_{t+1} - V^{S,k}_{t+1}) = 0, \tag{A12}$$

where infected individuals internalize the impact of their choices on all three groups, weighted by their respective shares S^k_t/N^k_t. The first-order conditions for the recovered individuals remain the same as in the baseline model, but now there is one for each group j.